Detecting gamma frequency neural activity using simultaneous multiband EEG-fMRI

Authors: Makoto Uji[a], Ross Wilson[a], Susan T. Francis[b], Karen J. Mullinger[a,b], Stephen D. Mayhew[a]

[a] Centre for Human Brain Health (CHBH), University of Birmingham, Birmingham, UK
[b] SPMIC, School of Physics and Astronomy, University of Nottingham, Nottingham, UK

Introduction

Multiband (MB) fMRI can provide shorter repetition times (TR), increased brain coverage [1,2], or shorter acquisition time in sparse fMRI which extends "quiet periods". Sparse MBfMRI has potential for improving simultaneous EEG recordings where residual gradient artefacts typically obscure gamma frequency neural activity [3,4]. This study aims to assess (1) the feasibility of simultaneous EEG-MBfMRI, both safety aspects related to the higher RF power of MB excitation and EPI image quality [5,6,7]; (2) the potential for investigating relationship between gamma activity and BOLD responses.

Methods

MRplus EEG amplifiers and 64-channel EEG cap (Brain Products) were used with a 3T Philips Achieva MRI scanner and MB acquisition (Gyrotools, Zurich).

Safety testing

The EEG cap was connected to an agar phantom. Fibre-optic thermometers (Luxtron) monitored the temperature of electrodes (ECG, Cz, TP7, FCz & TP8), cable bundle and scanner bore during two 20-minute scans (with MB=4 and SPIR fat suppression) testing the upper SAR limits: 1) GE-EPI (TR/TE=1000/40ms, slices=48, B1 RMS=1.09μT, SAR/head=22%); 2) PCASL-GE-EPI (TR/TE=3500/10 ms, slices=32, B1 RMS=1.58μT, SAR/head=46%).

Image quality

Data were recorded on 3 subjects during 5 GE-EPI sequences (Fig.1). Grey matter was segmented (FSL, FAST) from a T1 anatomical to mask the fMRI data. Image quality was assessed by comparing grey matter temporal SNR.

EEG-fMRI motor study

A trial involved 4 right-hand index finger abduction movements, auditory cued, within the MR quiet period, with a 16s baseline interval. 10 subjects completed 4 runs of 30 trials.

Data acquisition

EEG-fMRI were acquired using a sparse GE-EPI scheme (TR/TE=3000/40ms, MB=3, 33slices (acquisition time =0.75s, quiet period=2.25s), voxels=3mm^3, 192 volumes, SAR/head<7%). EMG was recorded from right first dorsal interosseous (FDI). A T1 anatomical and electrode locations were recorded (Polhemus Fastrak) for EEG source localization.

Data analysis

EEG

Gradient and pulse artefacts were corrected, data downsampled (600Hz) and epoched -16–2s relative to auditory cue onset (BrainVision Analyzer2). Trials contaminated with movement artefacts were removed. Eye-blinks/movements were removed (ICA, EEGLAB) and data were average referenced. A LCMV beamformer was employed with individual BEM head models (Fieldtrip [8]) to create T-stat images of changes in gamma (55–80Hz) power to finger abductions [active: 0–1.5s & passive: -9.0 to -7.5s windows]. A broadband (1-120Hz) timecourse of neural activity was extracted from the peak T-stat location in the contralateral motor cortex (cM1). Time-frequency spectrograms were calculated using multitaper wavelets [4]. The mean gamma power per trial (0-1.5s after auditory cue onset) formed a regressor for fMRI analysis.

fMRI

Data were motion corrected, smoothed (5mm) and normalised to the MNI template (FSL). First-level GLM analysis employed 2 regressors: 1) boxcar abduction movement, 2) parametric modulation of single-trial gamma activity, convolved with the HRF. Data were grouped over runs and then subjects (mixed effects).

Results

GE-EPI led to the greatest heating in the ECG channel (~0.5°) and nominal heating in other channels, with the higher SAR of the PCASL resulting in greater heating (ECG~0.9°). Heating levels were within safe limits, but highlight the increased heating dangers of EEG-MBfMRI due to increased B1 [9]. The variation in tSNR with MB and slice spacing was small (Fig.1).

Gamma EEG responses to FDI abductions (Fig.2a&b) localised to cM1. We observed both main-effect BOLD activation to the abductions and positive gamma-BOLD correlation in cM1 (Fig.2c). This correlation was focal to the central sulcus and motor hand-knob, supporting a tight coupling of natural variability in BOLD and gamma task responses [4,10].

Conclusions

These findings show the potential of EEG-MBfMRI for combined gamma activity and BOLD measures.

Figures

Multiband Factor	Slice acquisition spacing	tSNR
1	Equidistant	74 ± 40
2	Equidistant	72 ± 39
2	Sparse	67 ± 37
3	Equidistant	68 ± 37
3	Sparse	74 ± 38

Figure 1: Mean temporal SNR (tSNR) (±SD) calculated over grey matter across 3 participants during five MR sequences: MB: 1-3; acquisition type = equidistant or sparse. All other parameters were constant: TR/TE=3060/40ms, SENSE=2, slices=36, FA=79°, Volumes=41.

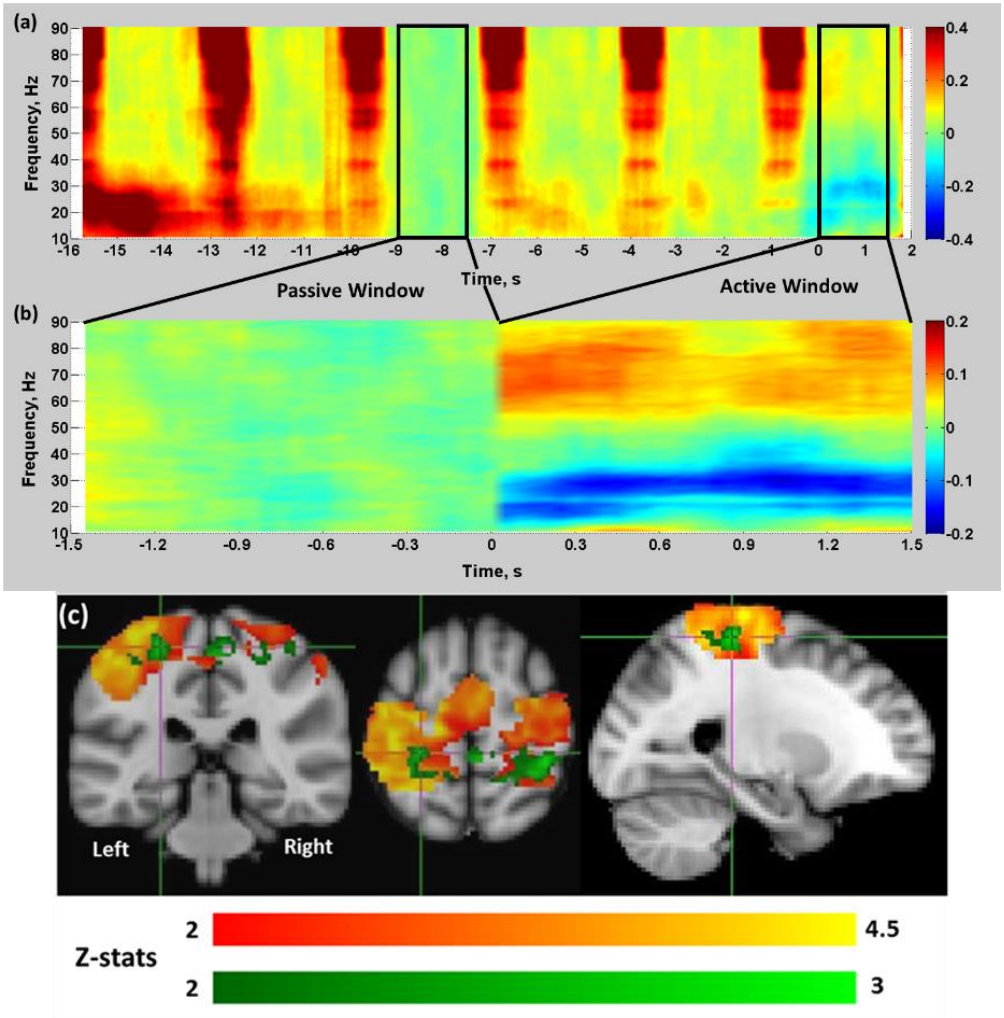

Figure 2: a) b) Mean time-frequency spectrograms from a representative subject demonstrating changes in the EEG signal power relative to the passive window (-9 to -7.5s). The passive window was located in an MR quiet period and before any anticipation of the stimulus. Time is displayed relative to the auditory cue onset. Spectrograms calculated with frequency resolution of 2.5Hz with spectral smoothing of ±10Hz. **a)** 18s whole-trial duration, note the residual gradient artefacts during fMRI acquisition periods. **b)** Gamma and beta power responses during the active window (0 to 1.5s) where movement occurred, with the passive window data appended pre-stimulus for comparison. **c)** Group average (N=10) fMRI mixed effects results. Main effect positive BOLD response to the right index finger abduction movements (red-yellow) and areas of positive correlation between single-trial EEG gamma and BOLD responses (green). Main effects and single-trial correlations are cluster corrected with $p<0.05$, masked with motor cortex.

References

1. Feinberg, D.A., et al., *Multiplexed echo planar imaging for sub-second whole brain FMRI and fast diffusion imaging.* PLoS One, 2010. **5**(12): p. e15710.
2. Moeller, S., et al., *Multiband multislice GE-EPI at 7 tesla, with 16-fold acceleration using partial parallel imaging with application to high spatial and temporal whole-brain fMRI.* Magn Reson Med, 2010. **63**(5): p. 1144-53.
3. Mullinger, K.J. and R. Bowtell, *Combining EEG and FMRI.* Methods in molecular biology (Clifton, N.J.), 2011. **711**: p. 303-26.
4. Scheeringa, R., et al., *Neuronal Dynamics Underlying High- and Low-Frequency EEG Oscillations Contribute Independently to the Human BOLD Signal.* Neuron, 2011. **69**(3): p. 572-83.
5. Auerbach, E.J., et al., *Multiband accelerated spin-echo echo planar imaging with reduced peak RF power using time-shifted RF pulses.* Magn Reson Med, 2013. **69**(5): p. 1261-7.
6. Mullinger, K., et al., *Effects of simultaneous EEG recording on MRI data quality at 1.5, 3 and 7 tesla.* Int J Psychophysiol, 2008. **67**(3): p. 178-88.
7. Chen, L., et al., *Evaluation of highly accelerated simultaneous multi-slice EPI for fMRI.* Neuroimage, 2015. **104**: p. 452-9.
8. Oostenveld, R., et al., *FieldTrip: Open source software for advanced analysis of MEG, EEG, and invasive electrophysiological data.* Comput Intell Neurosci, 2011. **2011**: p. 156869.
9. Collins, C.M. and Z. Wang, *Calculation of radiofrequency electromagnetic fields and their effects in MRI of human subjects.* Magn Reson Med, 2011. **65**(5): p. 1470-82.
10. Logothetis, N.K., *The underpinnings of the BOLD functional magnetic resonance imaging signal.* J Neurosci, 2003. **23**(10): p. 3963-71.

Acknowledgements

We thank the Birmingham-Nottingham Strategic Collaboration Fund for funding this research.